Investigation into hippocampal nerve cell damage through the mineralocorticoid receptor in mice

KENROH SASAKI and FUMIHIKO YOSHIZAKI

Department of Pharmacognosy, Tohoku Pharmaceutical University, Sendai, Miyagi 981-8558, Japan

Received May 15, 2014; Accepted February 17, 2015

DOI: 10.3892/mmr.2015.4406

Abstract. Stress-associated neuropsychiatric disease is associated with glucocorticoid levels; however, the behavior of mineralocorticoid receptors (MR) under conditions of stress remain to be elucidated. Steroid receptors in the brain are classified into glucocorticoid receptors (GR) and/or MR, exhibiting a difference in affinity for corticosteroids. The hippocampus is one of the most stress-susceptible regions in the brain. In the present study, it was investigated whether the two steroid receptors affect hippocampal neuron damage. The effect of fludrocortisones (FD) on hippocampal neurons caused by FD-containing cholesterol pellets subcutaneously embedded in the backs of mice (FD pellet group, 80 mg cholesterol and 20 mg FD) was investigated. A significant extension of the tail length by ~2.22 fold was observed in the FD pellet group compared with that in the control group as elucidated via the comet assay. Cytotoxicity (pyknosis and degranulation) and DNA fragmentation due to the death of nerve cells were observed using Kluver-Barrera staining and terminal deoxynucleotidyl transferase dUTP nick end labeling. Compared with the sham group mice, hippocampal neuron damage was observed in the adrenalectomized mice and the damage was suppressed by the combinatorial use of spironolactone, which suggested MR-induced hippocampal neuron damage. In conclusion, the present study clearly indicated a regional difference in vulnerability and/or sensitivity to corticosteroids. MR sensitivity to corticosteroids was high in the CA3 region and pyramidal cells of the hippocampus, which may therefore be vulnerable to corticosteroids. Thus, it is clearly suggested that MR function is important in the stress response.

Correspondence to: Professor Kenroh Sasaki, Department of Pharmacognosy, Tohoku Pharmaceutical University, 4-1 Komatsusima 4-chome, Aoba-ku, Sendai, Miyagi 981-8558, Japan
E-mail: kenrs@tohoku-pharm.ac.jp

Key words: stress, hippocampus, mineralocorticoid receptor, glucocorticoid receptor, comet assay, terminal deoxynucleotidyl transferase-mediated dUTP nick end labeling

Introduction

In recent years, stress-associated neuropsychiatric disorders have been increasing, and stress has become an important feature of modern society. Stress-associated neuropsychiatric disorders, including anxiety and post-traumatic stress disorder (PTSD), appear to be increasing. In the regulation of physiological function and response to stressful stimuli, the nervous, endocrine and immune systems are closely integrated. The hypothalamic-pituitary-adrenal axis (HPA axis) is a major feature of the neuroendocrine system, which controls reactions to stress. Steroid hormone production by the HPA axis increases in response to stressful stimuli, with the hypersecretion of corticoids contributing to stress-associated neuropsychiatric disease (1). Steroid receptors in the brain are classified into glucocorticoid receptors (GR) and/or mineralocorticoid receptors (MR). The hippocampus is one of the most stress-susceptible regions in the brain. GR and MR are abundant in the hippocampus (2). These receptors exhibit a difference in affinity for corticosteroids. GR are activated by stressful stimuli; however, MR are activated under physiological conditions. Blood glucocorticoid levels also increase in response to stressful stimuli; however, the behavior of MR under stress-induced conditions remains to be elucidated.

Therefore, an investigation was conducted with a focus on the following three points: MR are abundant in the hippocampus compared with other parts of the brain (3); the hippocampal CA regions exhibit significant cytotoxic atrophy, particularly in pyramidal cells in the CA3 region, due to social stress (4) and only MR are expressed in the CA3 region, whereas GR are not expressed (5). The aim of the present study was to develop novel treatment strategies for neuropsychiatric disease with impaired learning and memory functions and psychiatric disorders utilizing the hippocampal MR function.

Materials and methods

Drug treatment. Fludrocortisone (FD), aldosterone (Aldo), spironolactone (Spi), methyl green and diaminobenzidine (all from Sigma-Aldrich, St. Louis, MO, USA), cresyl violet acetate (MP Biomedicals, Illkirch, France) and Luxol Fast Blue (Chroma-Gesellschaft Schmidt and Co., Stuttgart, Germany) were used in the present study. Cholesterol, lithium

carbonate, pentobarbital sodium and sodium hydroxide were purchased from (Nacalai Tesque (Kyoto, Japan).

Animals. Male mice of the ddY strain (six weeks old) were obtained from Japan SLC Inc. (Hamamatsu, Japan) and maintained under a constant temperature and humidity (25±1˚C, 55±5% humidity) with a 12-h light/dark cycle (7:00 to 19:00, 19:00 to 7:00). Solid feed (CE-2, CLEA Japan Inc, Osaka, Japan) and hypochlorous acid water (10 ppm) were available *ad libitum*. The mice were acclimated to the environment for at least 1 week prior to the initiation of the experiment. Experiments were approved by the Institutional Animal Care and Use Committee of Tohoku Pharmaceutical University (Sendai, Japan) according to the guidelines for animal experiments prescribed by the Science Council of Japan.

After FD (20 mg) and cholesterol (80 mg) were pressed into tablets (0.5 mm^3/5 mm) using a tableting machine (Spectrum One, Perkin Elmer Co. Ltd., Waltham, MA, USA), these were embedded in mouse dorsal subcutaneous tissues for 1 week. Mice were sacrificed by decapitation. The right hippocampus was removed to collect the floating cells, then the left hippocampus was used to prepare the brain slices. The fresh and frozen tissues were placed in liquid nitrogen and then stored at -80˚C. An adrenalectomy was performed on a proportion of the mice under pentobarbital [60 mg/kg, intraperitoneally (i.p,)] anesthesia to remove the left and right adrenal glands followed by seven days of rearing.

Comet assay. The comet assay was performed using the CometAssay® kit (Trevigen, Gaithersburg, MD, USA). Briefly, following the collection of mouse hippocampal floating cells ($1x10^5$ cells/ml) via centrifugation at 300 x g for 10 min, agarose was added and the samples were sequentially subjected to alkaline lysis. Electrophoresis was performed at 50 V for 10 min, followed by the addition of SYBR green 1 nucleic acid stain. The gel was observed using a fluorescence microscope (Eclipse E-800, C1-LU3, C1-SHV; Nikon, Tokyo, Japan). Following capturing the PC image with Image Gauge version 4.0 (Fuji Photo Film Co. Ltd., Tokyo, Japan) on the fluorescence camera, the tail length was calculated to compare the cytotoxic intensity.

Preparation of cryostat sections. Sagittal sections (12 μm) were cut using a cryostat from the frozen samples of brain tissue embedded in cryomold optimum cutting temperature compound (Sakura Finetech Inc., Tokyo, Japan). The frozen blocks were sliced sequentially using a cryostat microtome (Microm HM505N; Microm International GmbH, Walldorf, Germany) to prepare serial sections. These sections were then mounted on (3-aminopropyl)triethoxysilane-coated micro slide glasses (Matsunami Glass Ind. Ltd., Tokyo, Japan) for assessment of the anatomical regions. Anatomical brain regions and brain areas were identified using a mouse brain atlas (6). The respective sections were maintained at -80°C until use.

Kluver-Barrera (KB) staining. After 20 min of air-drying at room temperature, the slices were incubated in 0.1% Luxol Fast Blue solution for 30 min at 60˚C, then washed successively in ethanol, lithium carbonate and deionized water. After the 90 min incubation at 37˚C in 10% cresyl violet acetate solution, the slices were washed in ethanol at 4˚C, followed by air-drying, then they were observed under an optical microscope (CX-41; Olympus Co. Ltd., Tokyo, Japan).

Terminal deoxynucleotidyl transferase (TdT) dUTP nick end labeling (TUNEL) staining. TUNEL staining was performed using the *in situ* apoptosis detection kit of Takara-Bio Inc. (Otsu, Japan). Briefly, the slices were fixed for 20 min in 4% formaldehyde solution and then the endogenous peroxidase was blocked in a 0.3% H_2O_2 methanol solution. Following incubation with the TdT enzyme (containing labeling safe buffer) in 50 μl/slice, the reaction adjustment solution (anti-fluorescein isothiocyanate-horseradish peroxidase conjugate) was added to the sample (70 μl/slice), followed by staining with 3,3'-diaminobenzidine-H_2O_2 solution. The counterstaining was performed with 3% methyl green solution.

Serum creatinine measurement. The Wako-Creatinine kit from Wako Pure Chemical Industry (Osaka, Japan) was used. The absorbance was measured at 492 nm (Immuno-mini, NJ-300; Biotec Co. Ltd., Tokyo, Japan) by addition of picric acid reagent and 0.75 M sodium hydroxide.

Statistical analysis. Values are expressed as the mean ± standard error of the mean. The Kruskal-Wallis analysis of variance rank test followed by Dunnett's test was performed to assess statistical significance using the Sigma Stat Statistical Software version 2.03 (Systat Software, Inc., Chicago, IL USA). $P<0.05$ was considered to indicate a statistically significant difference.

Results

MR exhibit an affinity for cortisol. MR are present in the cytoplasm of epithelial cells, producing an aldosterone-MR complex, which affects Na or water storage via movement into the nucleus. By contrast, cortisol is present at a concentration of ~1,000 times that of aldosterone in the blood, exhibiting a binding capacity equal to that of aldosterone for MR. The selective binding of MR and aldosterone in epithelial tissues, such as the kidney, is protected by type 2 11β-hydroxylase (11β-HSD2) (7), which rapidly converts cortisone to a low MR-affinity steroid, cortisol. MR have been revealed to be present in non-epithelial cells, including the brain and heart, and the levels of 11β-HSD2 in these organs are lower as compared with those in other epithelial tissues, particularly the hippocampus (8). Since cortisol cannot be converted to cortisone in the hippocampus, learning and memory disorders are caused by the excessive secretion of glucocorticoids in an acute stress disorder, such as PTSD. Therefore, it is possible that hippocampal neuron damage is not only due to the glucocorticoid-GR system, but is also regulated by the MR system. Based on this evidence, the effect of the administration of FD, a synthetic mineralocorticoid, on hippocampal neurons was investigated in mice. The effect of spironolactone on FD-induced hippocampal neuron damage *in vitro* was also examined.

Effect of FD on hippocampal neurons. The effect of FD on hippocampal neurons caused by embedding FD-containing

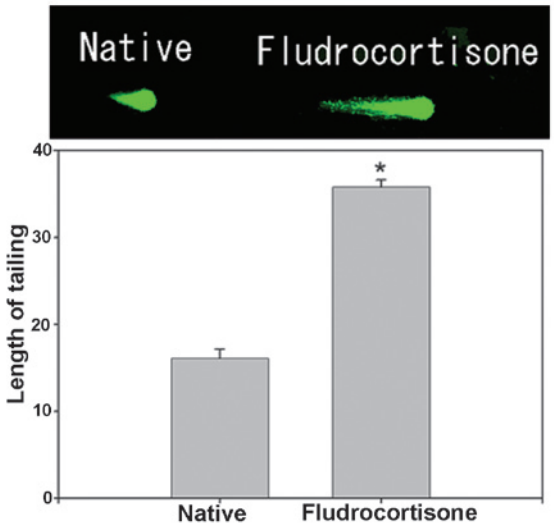

Figure 1. Effect of fludrocortisone on hippocampal floating cells in ddY mice (magnification, x400). Values are expressed as the mean ± standard error of the mean. Results are representative of the five animals evaluated (n=15 for each mouse; total, 75 per group). *P<0.05, compared with ddY mice.

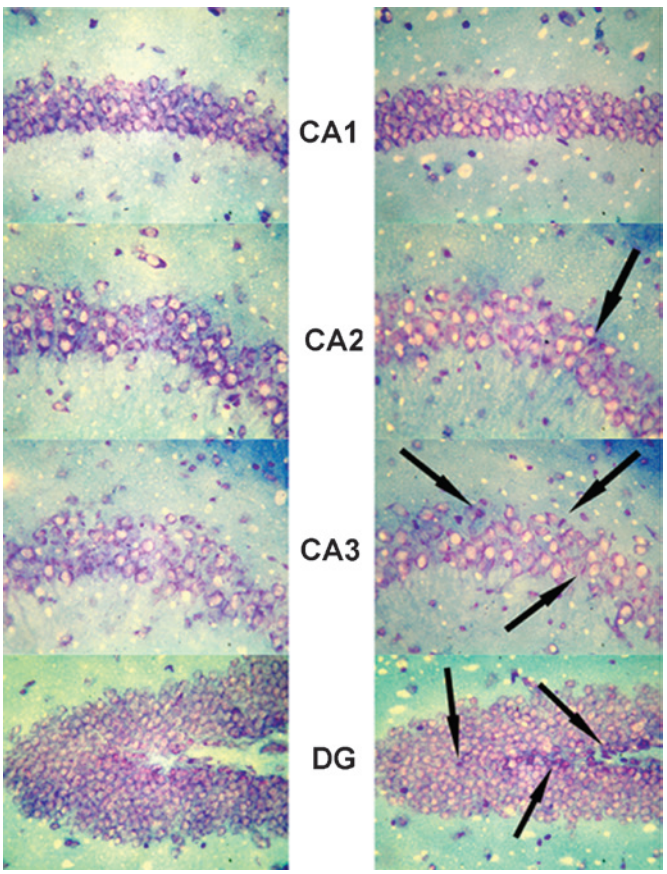

Figure 2. Neuronal damage of pyramidal cells and granule cells in mouse hippocampus following fludrocortisone administration (right) assessed by Kluver-Barrera staining (magnification, x100). Normal cells (left) have a round and pale appearance. Black arrows indicate the shrunken cells with pyknotic cells. DG, dentate gyrus.

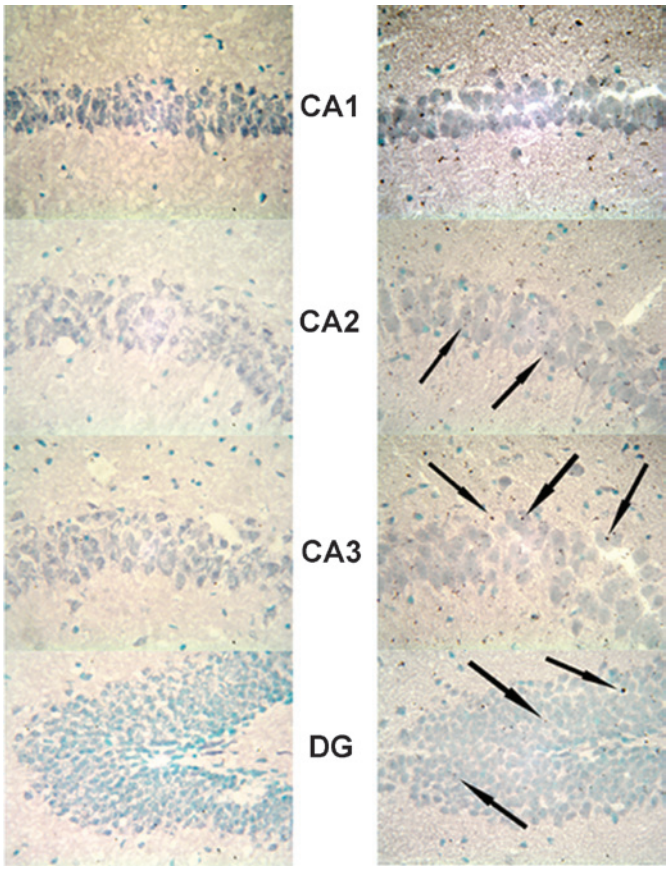

Figure 3. Increase of DNA fragmentation in mouse hippocampus following fludrocortisone administration (right) as compared with normal cells (left) as indicated by terminal deoxynucleotidyl transferase dUTP nick end labeling (magnification, x100). Surviving cells are indicated by light green or blue staining. Cells with DNA fragmentation exhibit a brown stain (black arrows). DG, dentate gyrus.

cholesterol pellets subcutaneously in the backs of mice (FD pellet group, 80 mg cholesterol and 20 mg FD) was investigated using the comet assay (n=15 for each mouse; total, 75 per group). A significant extension of the tail length by ~2.22 fold was noted in the FD pellet group compared with that in the control group (Fig. 1). Subsequently, morphological changes in hippocampal neurons based on KB staining and functional changes based on TUNEL staining were investigated.

Expression of MR in the hippocampus. In the hippocampus, MR numbers are equal to those of GR in the dentate gyrus (DG), CA1 and CA2 regions, but GR are absent in the CA3 region, where only MR are present (5). In the FD pellet group, cytotoxicity (pyknosis and degranulation) and DNA fragmentation due to the death of nerve cells were observed using the TUNEL method and KB staining in the CA3 region and DG, whereas the CA1 and CA2 regions barely exhibited cell damage (Figs. 2 and 3). It was clearly indicated that dysfunction of the hippocampal neurons is caused by MR, also showing differences in vulnerability and sensitivity to mineral corticoids in MR-containing regions in the brain. No significant difference was identified between the FD pellet and control groups regarding serum creatinine; thus, induction by hippocampal MR was suggested (Fig. 4).

Comet assay. Subsequently, the effect of Spi, an MR antagonist, and Aldo, an MR agonist, on normal mouse hippocampal floating cells was examined using the comet assay. No

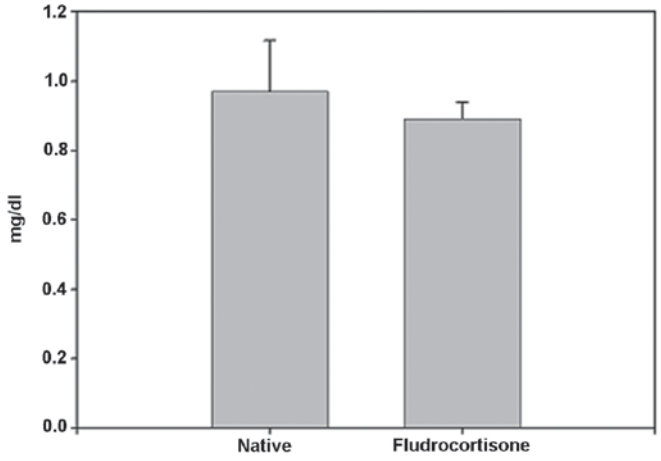

Figure 4. Effect of fludrocortisone on serum creatinine in mice. Values are expressed as the mean ± standard error of the mean. Results are representative of the five animals evaluated.

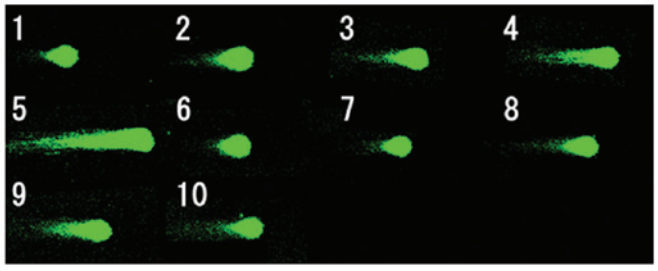

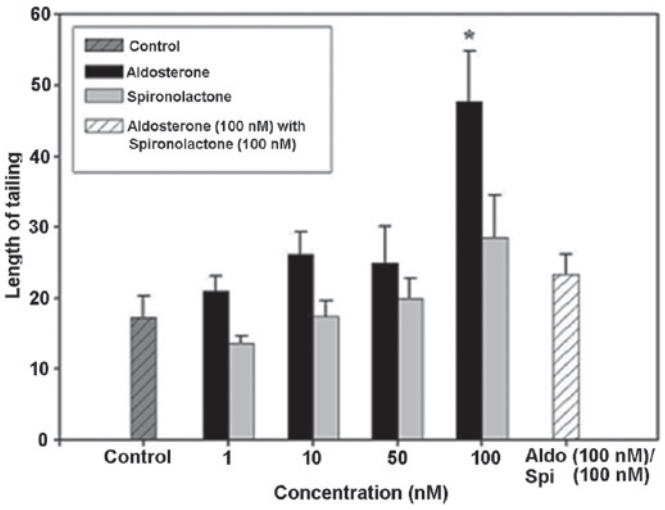

Figure 5. DNA damage in hippocampal floating cells caused by aldosterone and its inhibition by spironolactone (magnification, x400). Example of comet tail in floating hippocampal cells of (1) a native mouse, (2) with aldosterone 1 nM, (3) aldosterone 10 nM, (4) aldosterone 50 nM, (5) aldosterone 100 nM, (6) spironolactone 1 nM, (7) spironolactone 10 nM, (8) spironolactone 50 nM, (9) spironolactone 100 nM and (10) aldosterone 100 nM + spironolactone 100 nM. Values are expressed as the mean ± standard error of the mean (n=15 for each mouse; total, 75 per group). *P<0.05, compared with control value. Aldo, aldosterone; Spi, spironolactone.

significant difference was identified in the tail length compared with that of the control group following Spi addition alone. No significant difference was observed at 1, 10 or 50 nM with Aldo addition alone, but the tail length was extended by ~2.7 times compared with that in the control group at 100 nM (Fig. 5). The

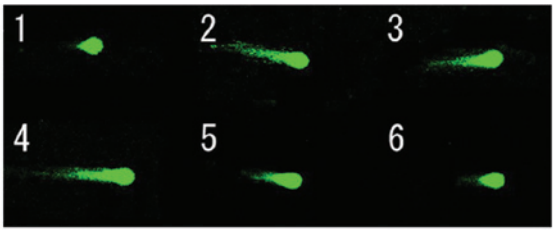

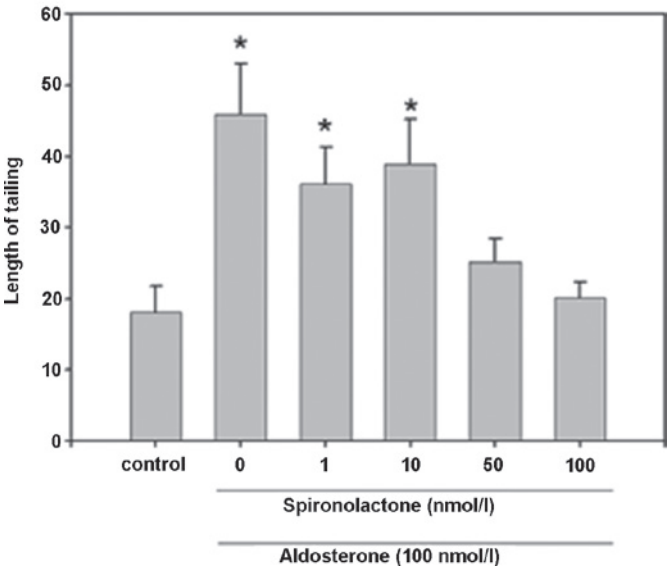

Figure 6. Concentration-dependent antagonism of spironolactone on aldosterone-induced mouse hippocampal neuronal dysfunction (magnification, x400). Example of comet tail in floating hippocampal cells of (1) a native mouse, (2) with aldosterone 100 nM, (3) aldosterone 100 nM and spironolactone 1 nM, (4) aldosterone 100 nM and spironolactone 10 nM, (5) aldosterone 100 nM and spironolactone 50 nM and (6) aldosterone 100 nM and spironolactone 100 nM. Values are expressed as the mean ± standard error of the mean (n=15). *P<0.05, compared with the control.

cytotoxicity of Aldo was suppressed by the addition of Spi, as in the combination group receiving Spi (100 nM) and Aldo (100 nM), the tail length was extended by ~1.3 times compared with that in the control group. Spi was added at increasing rates in addition to Aldo (100 nM), and the tail length in the combination group at was reduced to ~0.6 times and to ~0.3 times of that following Aldo treatment alone upon addition of 50 or 100 nM Spi, respectively (Fig. 6). Therefore, it was suggested that the cell damage caused by Aldo was induced through the action of the MR agonist and it may be suppressed by inhibiting MR.

Furthermore, the effect of FD (50 mg/kg, i.p.) and Spi (50 mg/kg, i.p.) on normal mouse hippocampal floating cells was examined using the comet assay with five mice in each group (n=15 for each mouse; total, 75 per group). In the present study, adrenalectomized (ADX) mice were used to eliminate the effects of endogenous corticosteroids (9), with the loss of the GR function in the hippocampus. While significant prolongation to ~2.88 times that of the control mice subjected to sham-surgery (Sham) was observed in the FD-administered group, the prolongation was inhibited by Spi alone by ~1.32- and 1.31-fold that in the FD group following concomitant administration of FD and Spi (Fig. 7). By contrast, although significant prolongation to ~1.96 times that in the control of ADX mice

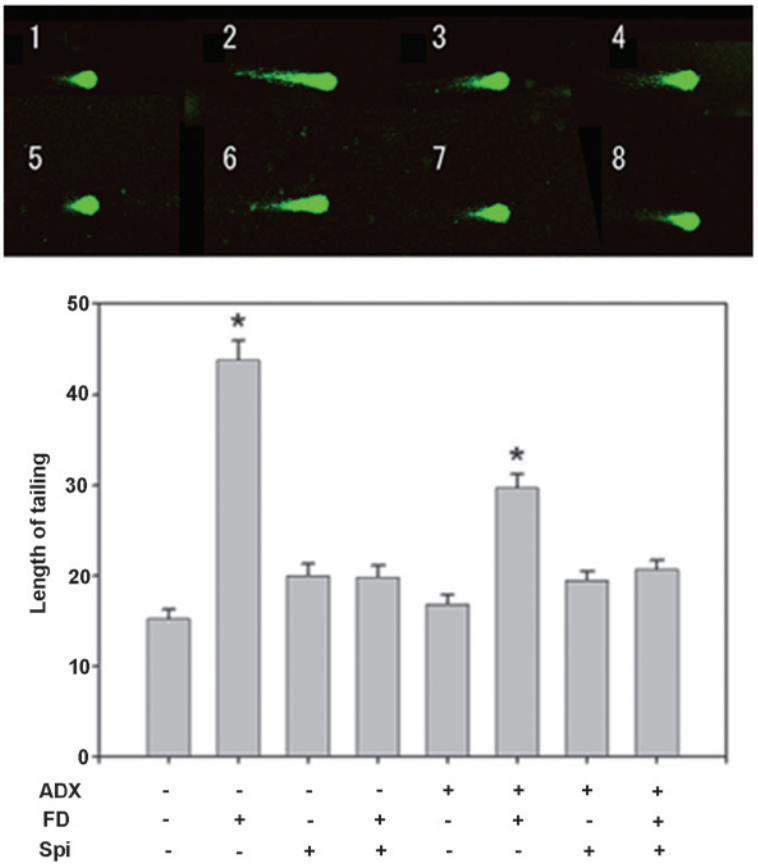

Figure 7. Effect of FD and Spi on hippocampal floating cells in adrenalectomized mice (magnification, x400). Example of comet tail of hippocampal floating cell of (1) a sham mouse, (2) FD 25 mg/kg s.c., bolus administration following sham surgery, (3) Spi 50 mg/kg i.p., bolus administration following sham, (4) FD 25 mg/kg s.c. and Spi 50 mg/kg i.p., bolus administration following sham, (5) ADX mouse, (6) FD 25 mg/kg s.c., bolus administration following ADX, (7) Spi 50 mg/kg i.p., bolus administration following ADX and (8) FD 25 mg/kg s.c. and Spi 50 mg/kg i.p., bolus administration following ADX. Values are expressed as the mean ± standard error of the mean. Results are representative of the five animals evaluated (n=15 for each mouse; total, 75 per group). *P<0.05, compared with control. Spi, spironolactone; FD, fludrocortisone; ADX, adrenalectomized; i.p., intraperitoneally; s.c., subcutaneous.

was observed in the FD-administered group, the prolongation was inhibited by Spi alone by ~1.11-fold and by FD and Spi administered concomitantly by 1.28-fold that in the FD group (Fig. 7). Thus, the FD-induced hippocampal neuronal disorder was suppressed by Spi in the ADX group, similarly to that in the Sham group. Subsequently, the morphological changes in hippocampal neurons caused by Spi administration and FD were examined via KB staining. No morphological changes were observed in the hippocampal neurons following FD administration in the ADX and Sham mice in the CA1 and CA2 regions (Figs. 8 and 9). The granule cells in the DG and pyramidal cells in the CA3 region did not exhibit granulation, pyknosis or dropout (Fig. 10B and F; Fig 11B and F). No significant difference was observed following Spi treatment alone, or with FD co-administered with Spi in the CA3 region (Fig. 10C, D, G and H; Fig. 11C, D, G and H). Furthermore, a TUNEL assay was employed to assess the functional changes in hippocampal neurons. DNA fragmentation was mildly observed in the CA1 and CA2 regions following FD treatment alone (Figs. 12B and 13B). However, marked fragmentation of DNA and neuronal cell death in the CA3 region and the DG were observed in the Sham group (Figs. 14B and 15B), while significant DNA fragmentation was noted only in the CA3 region and the DG when FD was administered alone to ADX mice. The was no observation of DNA fragmentation following Spi treatment alone (Figs. 14F and 15F), or co-administration of FD and Spi (Fig. 12C, D, G and H; Fig. 13C, D, G and H; Fig. 14C, D, G and H; Fig. 15C, D, G and H) in the Sham and ADX mice. Therefore, it is suggested that Spi inhibits hippocampal neuronal damage induced by administration of FD. Considering that an adrenalectomy causes the apoptosis of granule cells in the DG, following the promotion of neurogenesis (10), the turnover of granule cells in the DG should be increased in ADX mice to counteract cell loss.

Discussion

In addition to hippocampal neuron damage caused by the glucocorticoid-GR system, such damage may also be directly induced via MR by glucocorticoids or mineralocorticoids. As the affinity of glucocorticoids for MR is higher compared with that for GR (8) and low 11β-HSD2 levels exist in the hippocampus (11), GR and MR may be highly susceptible to an increase or decrease of glucocorticoids. However, GR are only activated to 30% with the minimum circadian concentration of glucocorticoids, but MR are activated to >60% in the hippocampus (12). With the spike of blood glucocorticoid levels due to acute stress, all MR are activated, but only 50% of GR are activated (12). Since, as well as in Sham mice, hippocampal neuron damage was observed following FD administration even in the

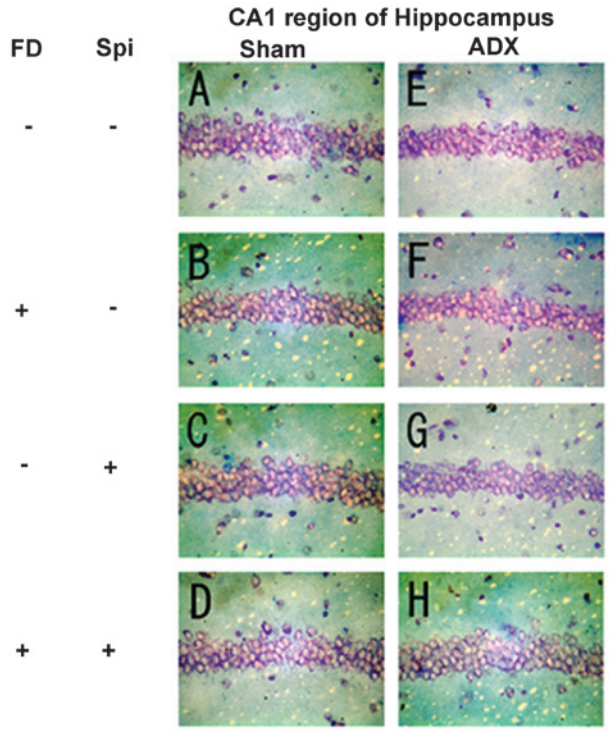

Figure 8. Effect of FD and Spi in the hippocampal CA1 region in adrenalectomized mice using Kluver-Barrera staining (magnification, x100). (A) Example of Kluver-Barrera-stained section of the hippocampus of sham group-mouse. (B) FD (25 mg/kg s.c.) bolus administration following sham surgery. (C) Spi (50 mg/kg i.p.) bolus administration following sham surgery. (D) FD (25 mg/kg s.c.) and Spi (50 mg/kg i.p.) bolus administration following sham surgery. (E) ADX mouse. (F) FD (25 mg/kg s.c.) bolus administration following ADX. (G) Spi (50 mg/kg i.p.) bolus administration following ADX. (H) FD (25 mg/kg s.c.) and Spi (50 mg/kg i.p.), bolus administration following ADX. Normal cells are indicated by the round and pale stain. Spi, spironolactone; FD, fludrocortisone; ADX, adrenalectomized; i.p., intraperitoneally; s.c., subcutaneous.

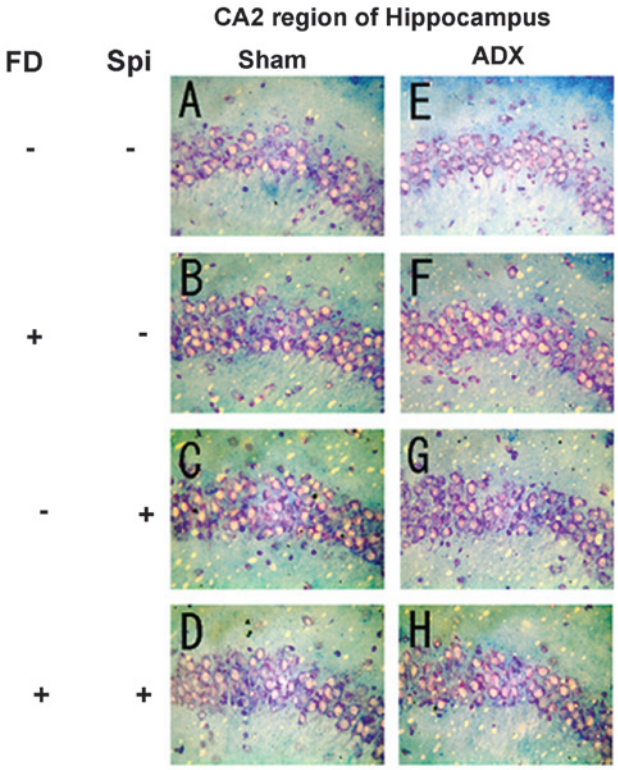

Figure 9. Effect of FD and Spi in the hippocampal CA2 region in adrenalectomized mice using Kluver-Barrera staining (magnification, x100). (A) Example of Kluver-Barrera-stained section of the hippocampus of sham group-mouse. (B) FD (25 mg/kg s.c.) bolus administration following sham surgery. (C) Spi (50 mg/kg i.p.) bolus administration following sham surgery. (D) FD (25 mg/kg s.c.) and Spi (50 mg/kg i.p.) bolus administration following sham surgery. (E) ADX mouse. (F) FD (25 mg/kg s.c.) bolus administration following ADX. (G) Spi (50 mg/kg i.p.) bolus administration following ADX. (H) FD (25 mg/kg s.c.) and Spi (50 mg/kg i.p.), bolus administration following ADX. Normal cells are indicated by the round and pale stain. Spi, spironolactone; FD, fludrocortisone; ADX, adrenalectomized; i.p., intraperitoneally; s.c., subcutaneous.

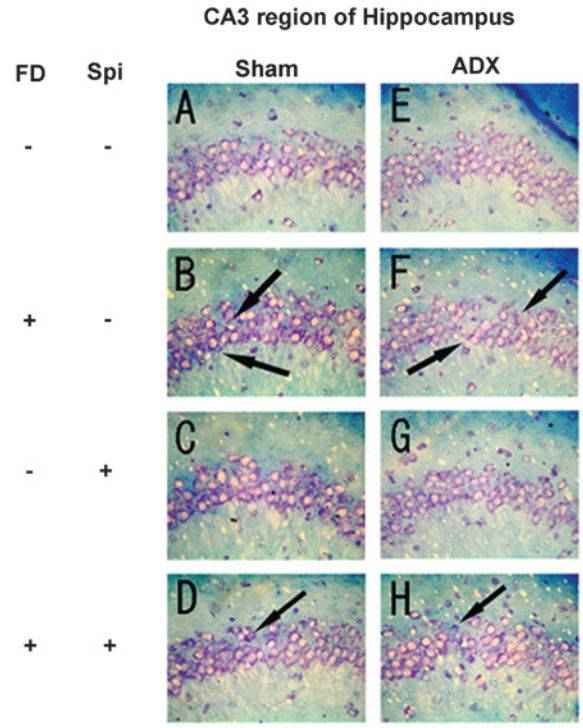

Figure 10. Effect of FD and Spi in the hippocampal CA3 region in adrenalectomized mice using Kluver-Barrera staining (magnification, x100). (A) Example of Kluver-Barrera stained section of the hippocampus of sham group-mouse. (B) FD (25 mg/kg s.c.) bolus administration following sham surgery. (C) Spi (50 mg/kg i.p.) bolus administration following sham surgery. (D) FD (25 mg/kg s.c.) and Spi (50 mg/kg i.p.) bolus administration following sham surgery. (E) ADX mouse. (F) FD (25 mg/kg s.c.) bolus administration following ADX. (G) Spi (50 mg/kg i.p.) bolus administration following ADX. (H) FD (25 mg/kg s.c.) and Spi (50 mg/kg i.p.), bolus administration following ADX. Normal cells are indicated by the round and pale stain. Spi, spironolactone; FD, fludrocortisone; ADX, adrenalectomized; i.p., intraperitoneally; s.c., subcutaneous.

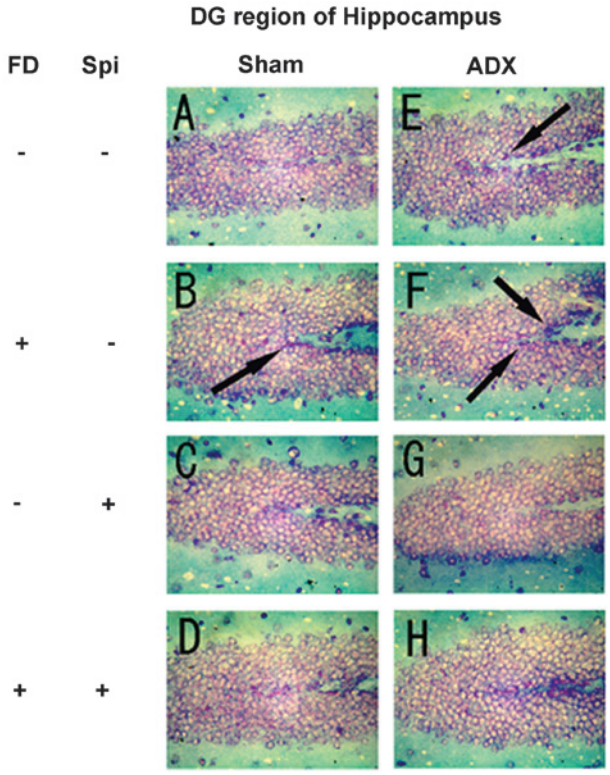

Figure 11. Effect of FD and Spi in the hippocampal DG in adrenalectomized mice using Kluver-Barrera staining (magnification, x100). (A) Example of Kluver-Barrera stained section of the hippocampus of sham group-mouse. (B) FD (25 mg/kg s.c.) bolus administration following sham surgery. (C) Spi (50 mg/kg i.p.) bolus administration following sham surgery. (D) FD (25 mg/kg s.c.) and Spi (50 mg/kg i.p.) bolus administration following sham surgery. (E) ADX mouse. (F) FD (25 mg/kg s.c.) bolus administration following ADX. (G) Spi (50 mg/kg i.p.) bolus administration following ADX. (H) FD (25 mg/kg s.c.) and Spi (50 mg/kg i.p.), bolus administration following ADX. Normal cells are indicated by the round and pale stain. Spi, spironolactone; FD, fludrocortisone; ADX, adrenalectomized; i.p., intraperitoneally; s.c., subcutaneous; DG, dentate gyrus.

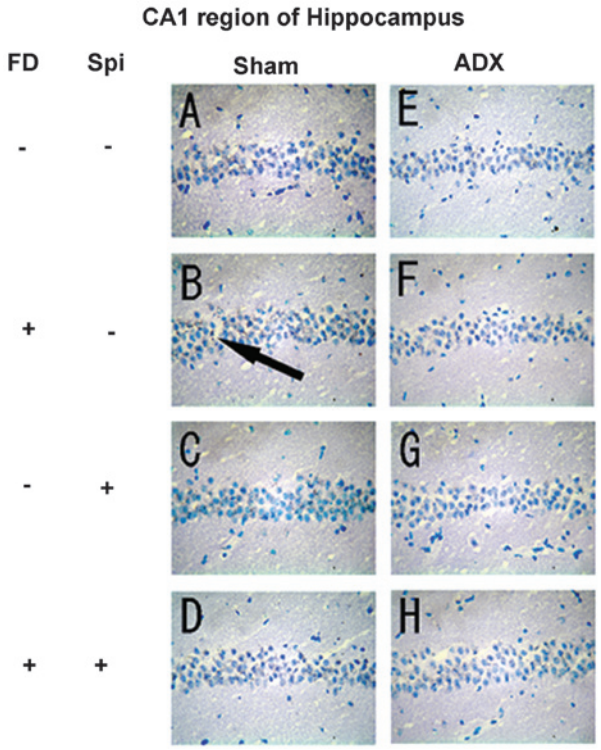

Figure 12. Effect of FD and Spi in the hippocampal CA1 region in adrenalectomized mice assessed using TUNEL staining (magnification, x100). (A) Example of TUNEL-stained section of the hippocampus of sham group-mouse. (B) FD (25 mg/kg s.c.) bolus administration following sham surgery. (C) Spi (50 mg/kg i.p.) bolus administration following sham surgery. (D) FD (25 mg/kg s.c.) and Spi (50 mg/kg i.p.) bolus administration following sham surgery. (E) ADX mouse. (F) FD (25 mg/kg s.c.) bolus administration following ADX. (G) Spi (50 mg/kg i.p.) bolus administration following ADX. (H) FD (25 mg/kg s.c.) and Spi (50 mg/kg i.p.), bolus administration following ADX. Normal cells are indicated by the round and pale stain. Spi, spironolactone; FD, fludrocortisone; ADX, adrenalectomized; i.p., intraperitoneally; s.c., subcutaneous; TUNEL, terminal deoxynucleotidyl transferase dUTP nick end labeling.

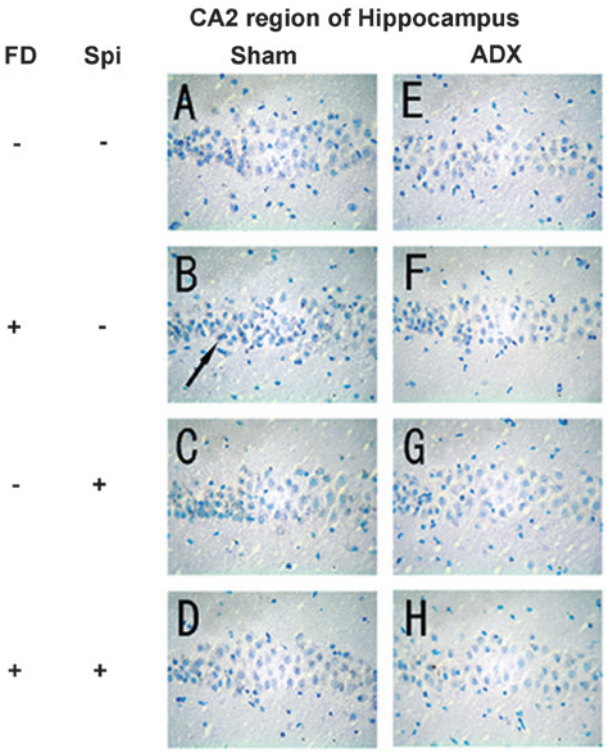

Figure 13. Effect of FD and Spi in the hippocampal CA2 region in adrenalectomized mice using TUNEL staining (magnification, x100). (A) Example of TUNEL-stained section of the hippocampus of sham group-mouse. (B) FD (25 mg/kg s.c.) bolus administration following sham surgery. (C) Spi (50 mg/kg i.p.) bolus administration following sham surgery. (D) FD (25 mg/kg s.c.) and Spi (50 mg/kg i.p.) bolus administration following sham surgery. (E) ADX mouse. (F) FD (25 mg/kg s.c.) bolus administration following ADX. (G) Spi (50 mg/kg i.p.) bolus administration following ADX. (H) FD (25 mg/kg s.c.) and Spi (50 mg/kg i.p.), bolus administration following ADX. Normal cells are indicated by the round and pale stain. Spi, spironolactone; FD, fludrocortisone; ADX, adrenalectomized; i.p., intraperitoneally; s.c., subcutaneous; TUNEL, terminal deoxynucleotidyl transferase dUTP nick end labeling.

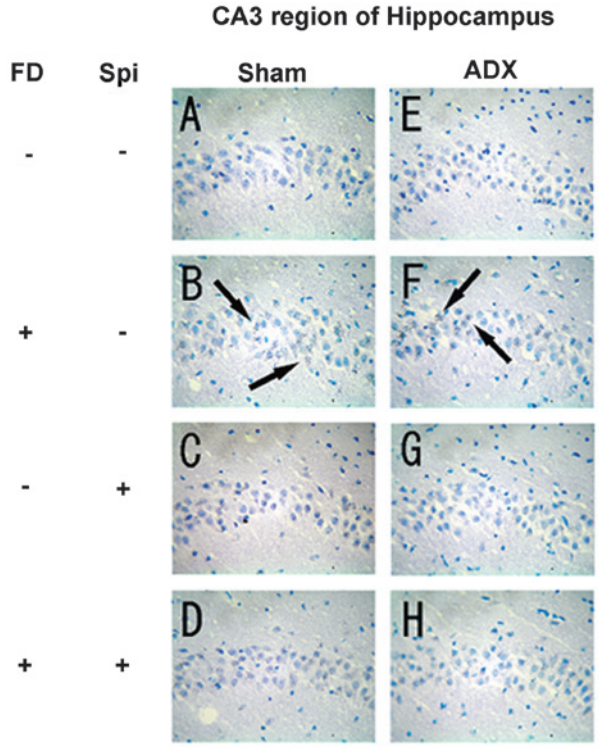

Figure 14. Effect of FD and Spi in the hippocampal CA3 region in adrenalectomized mice using TUNEL staining (magnification, x100). (A) Example of TUNEL-stained section of the hippocampus of sham group-mouse. (B) FD (25 mg/kg s.c.) bolus administration following sham surgery. (C) Spi (50 mg/kg i.p.) bolus administration following sham surgery. (D) FD (25 mg/kg s.c.) and Spi (50 mg/kg i.p.) bolus administration following sham surgery. (E) ADX mouse. (F) FD (25 mg/kg s.c.) bolus administration following ADX. (G) Spi (50 mg/kg i.p.) bolus administration following ADX. (H) FD (25 mg/kg s.c.) and Spi (50 mg/kg i.p.), bolus administration following ADX. Normal cells are indicated by the round and pale stain. Spi, spironolactone; FD, fludrocortisone; ADX, adrenalectomized; i.p., intraperitoneally; s.c., subcutaneous; TUNEL, terminal deoxynucleotidyl transferase dUTP nick end labeling.

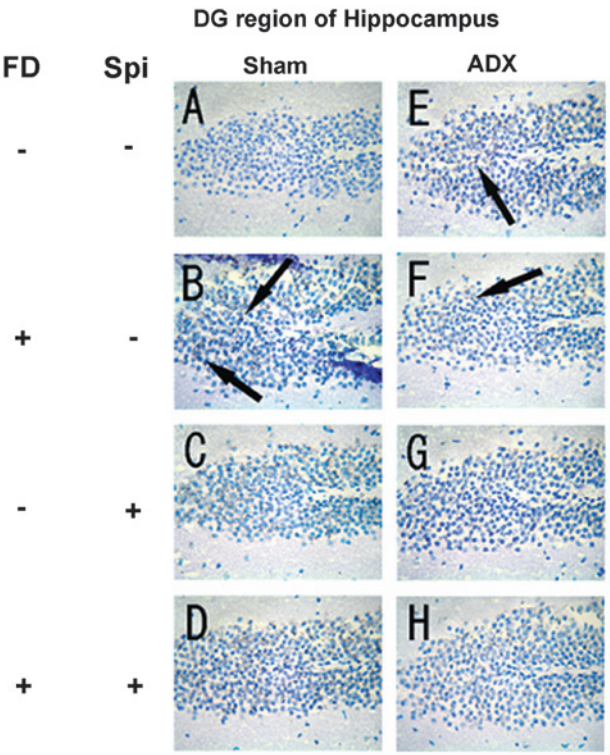

Figure 15. Effect of FD and Spi in the hippocampal DG in adrenalectomized mice using TUNEL staining (magnification, x100). (A) Example of TUNEL-stained section of the hippocampus of sham group-mouse. (B) FD (25 mg/kg s.c.) bolus administration following sham surgery. (C) Spi (50 mg/kg i.p.) bolus administration following sham surgery. (D) FD (25 mg/kg s.c.) and Spi (50 mg/kg i.p.) bolus administration following sham surgery. (E) ADX mouse. (F) FD (25 mg/kg s.c.) bolus administration following ADX. (G) Spi (50 mg/kg i.p.) bolus administration following ADX. (H) FD (25 mg/kg s.c.) and Spi (50 mg/kg i.p.), bolus administration following ADX. Normal cells are indicated by the round and pale stain. Spi, spironolactone; FD, fludrocortisone; ADX, adrenalectomized; i.p., intraperitoneally; s.c., subcutaneous; DG, dentate gyrus; TUNEL, terminal deoxynucleotidyl transferase dUTP nick end labeling.

ADX mice, and the damage was suppressed by the combined use with Spi, hippocampal neuron damage was suggested to be mediated via MR. In addition, these results clearly indicated the regional differences in vulnerability and/or sensitivity to corticosteroids of MR based on the TUNEL and KB staining assays. Since MR are only present in the CA3 region, MR sensitivity to corticosteroids in the CA3 region is expected to be high, and pyramidal cells are expected to be vulnerable to corticosteroids. An increase in the density of hippocampal MR following psychological stress has been reported (13). Further studies are required in the future to fully elucidate these functions.

In epithelial cells, MR form a complex with heat shock proteins (HSPs), following which they dissociate from the HSPs to form a dimer. Following dissociation from the HSPs, MR have been found to migrate into the nucleus from the cytoplasm, bind to the promoter region of the target gene with the MR response element and cause the transcriptional activation of target genes (14-16). However, the behavior of MR in non-epithelial cells, such as in the hippocampus, remains to be elucidated. Recently, it was reported that reactive oxygen species (ROS) were produced following the activation of nicotinamide adenine dinucleotide phosphate (NADPH) oxidase with increasing intracellular Ca^{2+} influx and lowering of the Mg^{2+} concentration by aldosterone binding to MR in non-epithelial cells, including the heart and blood vessels (17). Apoptosis has also been reported to be induced in heart tissue by Aldo loading in mice (18). In conclusion, hippocampal neuronal dysfunction may be caused by the overproduction of ROS induced by NADPH oxidase activation via MR functioning. In addition to hippocampal neuronal disorders caused by an MR agonist, the presence of disorders caused by an MR antagonist was hypothesized in the present study. In the clinic, organ-protective effects on the heart, blood vessels and non-epithelial tissue mediated by MR were shown to be inhibited by MR antagonists (19), clearly suggesting that MR function is important in the response to stress stimuli.

References

1. Sherin JE and Nemeroff CB: Post-traumatic stress disorder: The neurobiological impact of psychological trauma. Dialogues Clin Neurosci 13: 263-278, 2011.
2. Hwang IK, Yoo KY, Nam YS, Choi JH, Lee IS, Kwon YG, Kang TC, Kim YS, and Won MH: Mineralocorticoid and glucocorticoid receptor expressions in astrocytes and microglia in the gerbil hippocampal CA1 region after ischemic insult. Neurosci Res 54: 319-327, 2006.
3. Sánchez MM, Young LJ, Plotsky PM and Insel TR: Distribution of corticosteroid receptors in the rhesus brain: relative absence of glucocorticoid receptors in the hippocampal formation. J Neurosci 20: 4657-4668, 2000.
4. Sousa N, Lukoyanov NV, Madeira MD, Almeida OF and Paula-Barbosa MM: Reorganization of the morphology of hippocampal neurites and synapses after stress-induced damage correlates with behavioral improvement. Neuroscience 97: 253-266, 2000.
5. Han F, Ozawa H, Matsuda K, Nishi M and Kawata M: Colocalization of mineralocorticoid receptor and glucocorticoid receptor in the hippocampus and hypothalamus. Neurosci Res 51: 371-381, 2005.
6. Paxinos G and Franklin KBJ: The Mouse Brain in Stereotaxic Coordinates. Compact Third Edition. Academic Press, Waltham, 2008.
7. Funder JW: Mineralocorticoid receptors in the central nervous system. J Steroid Biochem Mol Biol 56: 179-183, 1996.
8. Connell JM and Davies E: The new biology of aldosterone. J Endocrinol 186: 1-20, 2005.
9. Hu Z, Yuri K, Ozawa H, Lu H and Kawata M: The in vivo time course for elimination of adrenalectomy-induced apoptotic profiles from the granule cell layer of the rat hippocampus. J Neurosci 17: 3981-3989, 1997.
10. Krugers HJ, van der Linden S, van Olst E, Alfarez DN, Maslam S, Lucassen PJ and Joëls M: Dissociation between apoptosis, neurogenesis, and synaptic potentiation in the dentate gyrus of adrenalectomized rats. Synapse 61: 221-230, 2007.
11. de Kloet ER: Hormones, brain and stress. Endocr Regul 37: 51-68, 2003.
12. Rogalska J: Mineralocorticoid and glucocorticoid receptors in hippocampus: their impact on neurons survival and behavioral impairment after neonatal brain injury. Vitam Horm 82: 391-419, 2010.
13. Ladd CO, Huot RL, Thrivikraman KV, Nemeroff CB and Plotsky PM: Long-term adaptations in glucocorticoid receptor and mineralocorticoid receptor mRNA and negative feedback on the hypothalamo-pituitary-adrenal axis following neonatal maternal separation. Biol Psychiatry 55: 367-375, 2004.
14. Pascual-Le Tallec L and Lombès M: The mineralocorticoid receptor: a journey exploring its diversity and specificity of action. Mol Endocrinol 19: 2211-2221, 2005.
15. Fuller PJ and Young MJ: Mechanisms of mineralocorticoid action. Hypertension 46: 1227-1235, 2005.
16. Connell JM and Davies E: The new biology of aldosterone. J Endocrinol 186: 1-20, 2005.
17. Sun Y, Zhang J, Lu L, Chen SS, Quinn MT and Weber KT. Aldosterone-induced inflammation in the rat heart: role of oxidative stress. Am J Pathol 161: 1773-1781, 2002.
18. Sam F, Xie Z, Ooi H, Kerstetter DL, Colucci WS, Singh M and Singh K: Mice lacking osteopontin exhibit increased left ventricular dilation and reduced fibrosis after aldosterone infusion. Am J Hypertens 17: 188-193, 2004.
19. Pitt B, Zannad F, Remme WJ, Cody R, Castaigne A, Perez A, Palensky J and Wittes J; Randomized Aldactone Evaluation Study Investigators: The effect of spironolactone on morbidity and mortality in patients with severe heart failure. N Engl J Med 341: 709-717, 1999.